AN EFFICIENT CIRCULAR CONTACT GRID FOR CONCENTRATOR SOLAR CELLS

V. M. ANDREEV, R. ROMERO* and O. V. SULIMA

A. F. Ioffe Physico-technical Institute, Academy of Sciences of the U.S.S.R., Leningrad (U.S.S.R.)

(Received September 22, 1982; accepted September 6, 1983)

Summary

Efficient circular contact grids are developed for solar cells intended for work at high levels of concentrated sunlight. The cell efficiency is studied as a function of grid design, concentration ratio and cell radius. It was found that there is a trade-off between the maximum cell efficiency and the decay in the efficiency as a function of concentration. For $Al_xGa_{1-x}As$–GaAs cells 15 mm in diameter a high efficiency may be achieved even at a concentration of over 300-fold with a shading loss as low as 5%. For a concentration of 800 suns, good results may be obtained at about 10% shading.

At 800 suns, doubling the cell diameter from 1 to 2 cm accounts for less than a 2% loss in cell efficiency, and this loss in efficiency is primarily related to the power loss due to increased current flow through the grid towards the outer collector.

1. Introduction

Efficient conversion of concentrated sunlight is one of the most promising approaches towards the achievement of cheap solar electricity [1 - 8].

It is a well-established fact in concentrator solar cell design that minimum resistance plus shading losses lead to maximum efficiencies. In typical $Al_xGa_{1-x}As$–GaAs devices the Joule loss is mainly due to the front p-type layer sheet resistance and the power drop on the contact grid. Special care has been taken to reduce the sheet resistance (without curtailing the spectral response), improving the diffusion lengths in the thick epitaxial GaAs layers [3, 8] by enhancing the thin p-type layer conductivity via vapour phase zinc diffusion [9] or beryllium diffusion [5, 6].

Nevertheless, only recently have there been any attempts to minimize the Joule loss and the shading power drop at the concentrator cell contact

*On leave from Havana University, Havana, Cuba.

0379-6787/84/$3.00 © Elsevier Sequoia/Printed in The Netherlands

grid through efficient grid design based on an extension of classical 1 sun patterns [10, 11]. In ref. 6 the circular contact grid configuration was designed using a computer modelling program and high conversion efficiencies of concentrated (up to 1000 suns) sunlight were achieved, but no discussion of grid design results and design procedure was given. It is the purpose of this paper to discuss the development of effective front-contact grid designs for solar cells intended for work under high current generation conditions.

2. Grid design procedure

In high concentration systems the light spot is usually a circle; thus circular symmetry is assumed to be the natural symmetry of concentrator solar cells. Among the many possible grid configurations, that shown in Fig. 1 was chosen as the basic design because of its simplicity (only two different contact levels are involved) and because it may effectively relieve any anomalous current collection arising from local contact failure through the thick equipotential concentric collectors.

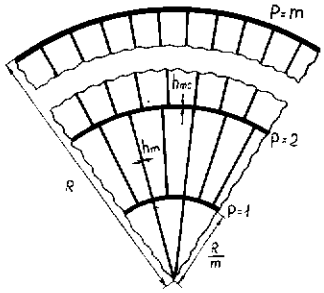

Fig. 1. The grid design under consideration. Radial fingers of width h_m are uniformly distributed between adjacent metal collectors of width h_{mc}. The collectors are R/m apart where m is the total number of collectors and R is the cell radius; p is the collector order number.

The spatial distribution of the incident light concentrated by the mirror was measured on the cell plane (17 mm in diameter). It was found that 80% of the cell plane was illuminated uniformly. A satisfactory uniformity of the spatial distribution of the light transmitted by the concentrating lens was also found in the work reported in ref. 6. Thus we assumed a uniform distribution of the light intensity on the whole cell plane.

Low loss grids are generated by choosing the number of concentric collectors and the number of metal fingers (linking adjacent collectors) that minimize ohmic and shading losses in the device at a given concentration level K.

Ohmic losses are taken as the power drops due to current flow through the semiconductor layer, the metal–semiconductor interface and the metal grid.

The power drop due to current flow through the semiconductor layer is calculated in each portion of the cell located between two adjacent radial fingers, and annular collectors do not contribute to current collection. The Joule loss is taken as the product of the square of the current flowing towards the metal finger at each point of the layer and the electrical resistance that this current faces. If it is assumed that in the portion (ring) of the solar cell located between collectors p and $p-1$ there are a total of N_p radial fingers linking these collectors, then the Joule loss due to current flow across this layer is

$$P_s = \frac{2KJ_L{}^2\rho_s R^2\pi^2\{p^4-(p-1)^4\}}{3P_0 h_s m^4}\frac{1}{N_p{}^2}$$

$$= \frac{\lambda_{sp}}{N_p{}^2} \qquad (1)$$

where m is the total number of annular collectors within the cell and p is the collector order number. The rest of the parameters involved appear in Table 1. Equations (1) - (4) are explained in Appendix A.

TABLE 1

Numerical data involved in the calculations

Parameter	*Value*
Photogenerated current density J_L	2.675×10^{-2} A cm^{-2}
Incident power density (air mass 1.2) P_0	8.14×10^{-2} W cm^{-2}
Metallization specific resistance ρ_m	2×10^{-6} Ω cm
Semiconductor specific resistance ρ_s	1×10^{-3} Ω cm
Contact specific resistance ρ_c	5×10^{-5} Ω cm^2
Metal finger width h_m	1×10^{-3} cm
Metal finger height t_m	5×10^{-4} cm
Metal collector width h_{mc}	2.5×10^{-3} cm
Cell radius R	0.75 cm
p-GaAs layer height h_s	1×10^{-4} cm
Junction saturation current density J_0	2×10^{-19} A cm^{-2}
Junction perfection factor A	1
Temperature T	298 K

Before flowing across the metal contact grid the current collected through the semiconductor layer gives rise to a power loss at the semiconductor–metal interface. This power loss is calculated as the product of the square of the collected current and the contact resistance (the specific contact resistance multiplied by the inverse contact area). For the N_p radial fingers located between collectors p and $p-1$ the contact resistance power loss is

$$P_c = \frac{KJ_L^2 R\rho_c \pi}{P_0 h_m} \frac{4}{m^3}\{p^2-(p-1)^2\}^2 \frac{1}{N_p}$$

$$= \frac{\lambda_{cp}}{N_p} \tag{2}$$

The current collected at the semiconductor–metal interface between collectors p and $p-1$ then flows along the radial fingers towards the outermost collector. The total current within the cell rings between collectors of lower p values flows together with this current. The current density along the radial fingers is a very strong function of position. The Joule loss due to current flow along the metal fingers is thus the product of the square of the total current flowing along the finger at each point and the metal finger resistance. For the N_p fingers this amounts to

$$P_m = \frac{KJ_L^2 \rho_m R^3 \pi}{P_0 h_m t_m}\left\{\frac{(p-1)^4}{m^5} + 4g(p)\right\}\frac{1}{N_p}$$

$$= \frac{\lambda_{mp}}{N_p} \tag{3}$$

where

$$g(p) = \frac{1}{m^5}\left[\frac{p^5-(p-1)^5}{5} - \frac{2(p-1)^2\{p^3-(p-1)^3\}}{3} + (p-1)^4\right]$$

In contrast, the power loss within the cell due to the area shaded by the N_p fingers between collectors p and $p-1$ is

$$P_{sh} = \frac{h_m N_p}{\pi R m}$$

$$= \lambda_{shp} N_p \tag{4}$$

In all cases the power losses have been normalized to the total incident power on the cell, namely $P_0 \pi R^2 K$.

Contact grid design is based on the minimization of the total Joule loss plus shading loss in each ring. Grid design consists in establishing the correct number of radial fingers linking two adjacent collectors and the total number of annular collectors needed to achieve a minimum power loss at a given concentration level. The number of radial fingers leading to a minimum power loss in the ring between collectors p and $p-1$ is obtained by using the fact that $d(P_s + P_c + P_m + P_{sh}) = 0$ which yields

$$(\lambda_{mp} + \lambda_{cp})\frac{1}{N_p^2} + 2\lambda_{sp}\frac{1}{N_p^3} - \lambda_{shp} = 0 \tag{5}$$

It is thus straightforward to find the total power loss in the cell from the solution of eqn. (5) for different values of p. The appropriate number of annular collectors is established by comparison of the respective total power losses for different configurations. Care is taken everywhere to include the collector shading.

3. Grid performance evaluation

Under high concentrations the current at the point of maximum solar cell power output is quite different from the cell photogenerated current. In consequence, a simple relation between the total power loss and the cell efficiency at a given level of injection may not be established. In order to describe the cell behaviour better it is useful to study the cell conversion efficiency which is taken to be the ratio of the maximum output power delivered by the device to the total incident power.

The point of maximum power output of the cell is calculated from the current–voltage (I–V) characteristic of the cell for the case in which the distributed character of the series resistance is not taken into account (the lumped parameter model), *i.e.* from

$$I = KJ_L(1 - P_{sh})\pi R^2 - J_0\pi R^2\left[\exp\left\{\frac{q(V + IR_s)}{AK_BT}\right\} - 1\right] \tag{6}$$

where P_{sh} is the total cell shading loss, A the junction perfection factor, K_B the Boltzmann constant and T the temperature. R_s is an effective series resistance which is introduced as the ratio of the total cell ohmic power loss $P_s + P_c + P_m$ to the square of the total current generated within the cell. It is found that such a resistance is not dependent on the current level and reproduces the experimental data quite well.

The cell efficiency is thus given by

$$\eta = \frac{I_m V_m}{\pi R^2 K P_0} \tag{7}$$

where I_m and V_m are the current and voltage respectively at the point of maximum power delivery.

In order to check the validity of this method, efficiency measurements were performed at different illumination levels on a thick window p-$Al_{0.7}$-$Ga_{0.3}As$–p-GaAs–n-GaAs–n^+-GaAs cell 17 mm in diameter with a contact grid of the kind shown in Fig. 1 and with three collectors which have 76, 154 and 244 fingers. The solar cells of this kind were manufactured before our calculations and thus had no optimized contact grid configuration. The finger and circular collector width was 30 μm while the metallization height was 23 μm. The measured sheet resistance of the p-type region (p-$Al_{0.7}Ga_{0.3}$

and p-GaAs layers) was 21.5 Ω/□ and the thickness was 30 μm. The specific resistance of the metallization (indium) was taken to be 9.03×10^{-6} Ω cm and the contact specific resistance was 5×10^{-5} Ω cm^2. The measured cell dark current density was 2×10^{-19} A cm^{-2} and the junction perfection factor A was 1. The experimental efficiencies were compared with the efficiencies calculated using the lumped parameter solar cell equivalent circuit of eqn. (6). The effective series resistance R_s calculated as described above, was 3.57 mΩ. As a result, at air mass 1.2 concentration levels of 943, 2281, 3421 and 4561 suns the measured efficiencies were 19.0%, 16.5%, 12.8% and 10.9% respectively and the calculated values, 20.2%, 16.6%, 13.6% and 11.0% respectively, are in good agreement with these measured values. Thus this method of solar cell efficiency calculation can be used for solar cells with various circular grid configurations including concentric collectors and radial metal fingers. The $I-V$ characteristic parameters corresponding to high concentration levels were obtained with the help of a xenon flash lamp. The measured values of open-circuit voltage (corresponding to the respective values of sunlight concentration levels mentioned above) were 1.15 V, 1.165 V, 1.17 V and 1.17 V and the fill factors were 0.86, 0.74, 0.57 and 0.49. The deviation from the measured efficiencies is due primarily to the assumption of one resistance value in the lumped parameter model. In general, an even better fit is possible if the lumped and distributed resistances are taken separately as two effective values in a distributed parameter equivalent circuit as developed in ref. 12.

The numerical data used for the calculations appear in Table 1. The incident power P_0 at 1 sun is calculated utilizing the data in ref. 13. Using the notation of ref. 13, the calculations are performed under S conditions (a clear cool (15 °C) summer day with air mass 1.2) and only the DF sunlight component (the direct component plus the Mie component (due to the scattering of sunlight at aerosols)) is taken into account, because it is the only component that is relevant under concentrated sunlight. The photogenerated current density J_L is integrated by matching the DF-S spectral distribution with the calculated spectral response of an $Al_xGa_{1-x}As$–GaAs cell with an ultrathin (hundreds of ångströms thick) window. The spectral response is found to be approximately a rectangle of 0.9 collection efficiency in the 300 - 850 nm range.

The 10^{-3} Ω cm p-GaAs specific resistivity is achieved with the help of vapour phase zinc diffusion through the $Al_xGa_{1-x}As$ layer [9] which allows for the very low sheet resistance without curtailing the spectral response. This result can be explained by the existence of the built-in electric fields which appear as the result of the hole concentration gradient in the p-GaAs layer after zinc diffusion; the hole concentration p changes from 10^{20} cm^{-3} near the heterojunction to 5×10^{17} cm^{-3} at the p–n junction. These electric fields considerably increase the effective diffusion length values of minority carriers in the p-GaAs layer in comparison with the case in which the p-GaAs layer has the same maximum hole concentration but no concentration gradient.

4. Results and discussion

Four efficient contact grid designs are generated for work at different concentration (current injection) levels. They are the minimum power loss contact grid designs for insolations of 66, 330, 662 and 3310 suns. Their specifications appear in Table 2. In Fig. 2 the cell efficiency η is calculated as a function of the concentration level K. It can be seen that each design is advantageous in a specific concentration range and that there is a trade-off between the maximum efficiency and the decay in the efficiency as the amount of shading increases and as the effective resistance decreases for high K designs (see Table 2). To assess the efficiency loss related to the contact grid, the ideal cell efficiency (which neglects the ohmic and shading losses) is plotted.

TABLE 2

Contact grids designed for high conversion efficiencies

Device	*Number of collectors*	*Number of fingers per ring*	*Effective series resistance* (mΩ)	*Shading loss* (%)
I	2	18, 52, 93	19.3	3
II	3	25, 71, 126, 193	8.3	5.4
III	4	26, 72, 126, 191, 271	5.9	7.2
IV	5	41, 119, 207, 311, 439, 594	3	13.8

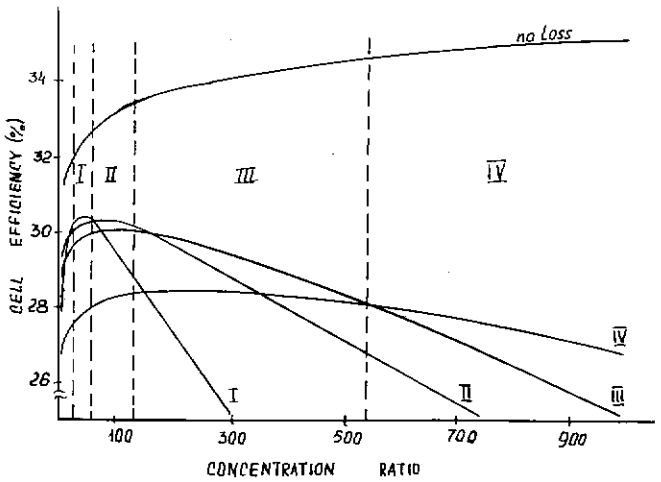

Fig. 2. Cell efficiency η *vs.* concentration ratio K for the grid designs shown in Table 2. The loss-less cell efficiency is also shown. The vertical broken lines indicate the intervals in which a specific grid design is advantageous.

The component power losses are plotted as a function of K for device III in Fig. 3. The linear rise in power loss (Fig. 3, curve PKT) results in a non-linear decay in cell efficiency due to the change in current at the point of maximum power output. As expected, the power loss due to current flow through the cell metallization is the main source of Joule dissipation for any K, although contact loss is also important. As can be seen, no simple relations can be established between the ohmic component losses and the shading to serve as guidelines in grid design as has been possible for low injection devices [10].

As can be noted from Fig. 4 (device III; $K = 662$), the power loss within the outer portion of the cell (ring 5) is of greatest importance. This is true because all the current is drained towards the outer collector. A better balance between the ohmic losses in the different rings might give a more efficient grid design as it should reduce the cell series resistance without a great increase in shading. This could be achieved if thicker fingers were inserted between the outer metal collectors.

An evaluation of the importance of the number of collectors in cell performance is shown in Fig. 5. Devices with minimum power loss were designed for work at $K = 662$ with different numbers of inner collectors

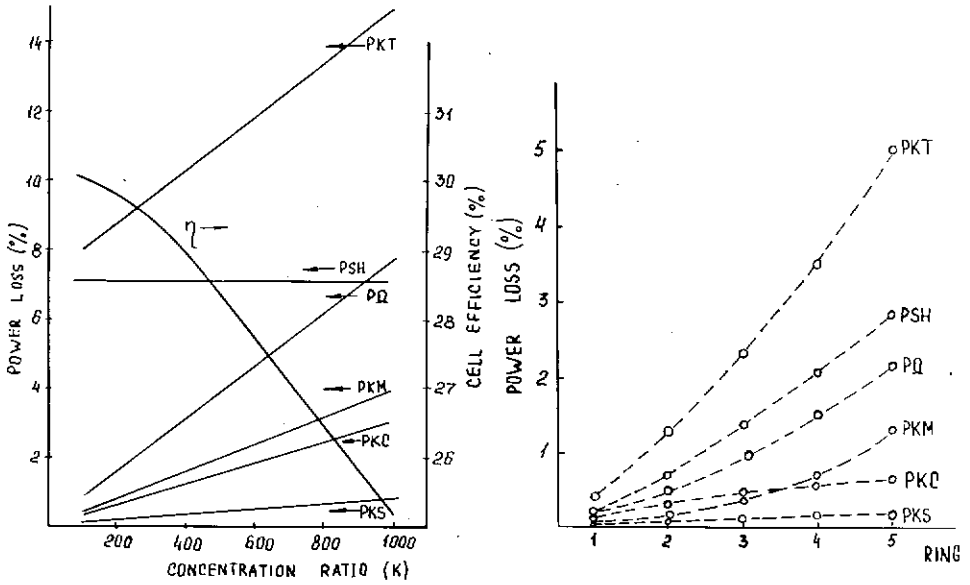

Fig. 3. Power loss (left scale) and cell efficiency (right scale) for device III: curve PKS, the Joule loss due to current flow through the semiconductor; curve PKC, the Joule loss due to the metal–semiconductor interface; curve PKM, the Joule loss through the metal grid; curve PΩ (equal to curve PKS plus curve PKC plus curve PKM), the total ohmic loss; curve PSH, the shading loss; curve PKT (equal to curve PSH plus curve PΩ), the total loss; curve η, cell efficiency.

Fig. 4. Component Joule and shading losses for the rings between adjacent collectors in device III at $K = 662$. The meanings of the curve labelling are as in Fig. 3.

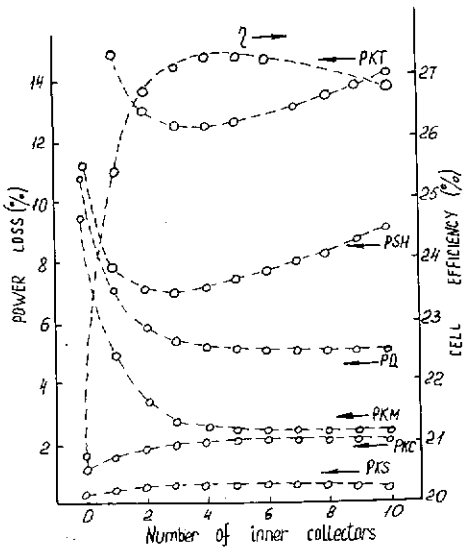

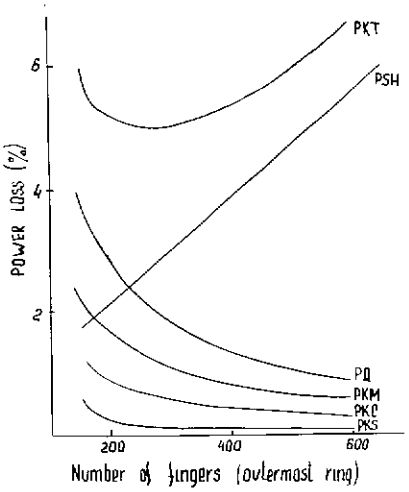

Fig. 5. Power loss (left scale) and cell conversion efficiency (right scale) for grid designs with different numbers of annular collectors at $K = 662$. The meanings of the curve labelling are as in Fig. 3.

Fig. 6. Power loss for the outermost ring of a type III device at $K = 662$. The meanings of the curve labelling are as in Fig. 3.

(from 0 to 10). An increase in the number of collectors saturates the ohmic losses at the expense of excessive shading; hence a minimum total power loss is observed for four inner collectors (device III). Correspondingly, the maximum cell efficiency is also attained in such a design because it allows for both minimum shading and series resistance. Nevertheless, the efficiency maximum is quite broad. Increasing the number of collectors from four to ten reduces the cell efficiency by only 0.52% while, from the point of view of cell fabrication and performance, designs with a larger number of thick metal collectors and a smaller number of thin metal fingers may be desirable.

A similar analysis is true for the number of fingers between the metal collectors. In Fig. 6 the number of fingers in the outermost ring of device III changes from 150 to 600 and the component power losses are calculated at $K = 662$. As above, an increase in the metallization tends to saturate the ohmic losses at the expense of increased shading. Thus, the minimum total power loss occurs when the number of fingers is about 271 as in device III. This minimum is also quite wide. A reduction in the number of fingers from 271 to 200 causes an increase in the total power loss of only 0.2%, and such a reduction might be technologically advisable.

The influence of the cell radius on the cell efficiency can be seen in Fig. 7 for a concentration level of 813 suns. The efficiencies related to designs are shown with maximum efficiency at $K = 813$ and in all cases the grids are optimized for a minimum loss at $K = 3310$. An increase in the cell radius slowly reduces the efficiency in the 0.5 - 1 cm region, while the total

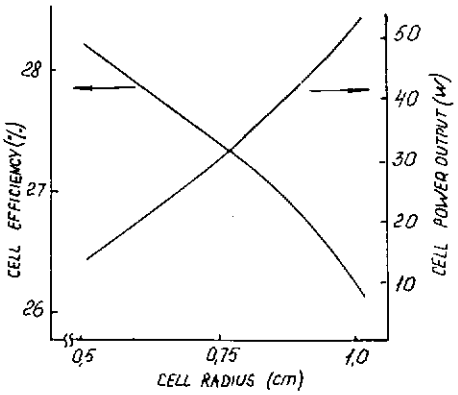

Fig. 7. Cell conversion efficiency (left scale) and cell power output (right scale) as a function of radius for grid designs with a maximum efficiency at $K = 813$.

power that the cell delivers rises quite steeply. The choice of optimum cell radius depends mostly on the design of the concentrator system. If a fixed temperature is achieved through external cooling, then the limiting factor in increasing the cell radius might be the concentrator optics. In contrast, for completely autonomous concentrator systems [4] an increased cell radius might be limited by heat sinking.

5. Conclusions

The power loss in the front metal contact grid of a concentrator solar cell leads to a substantial reduction in the cell efficiency. For a type IV device (Fig. 2) the grid-related losses amount to an 8.32% reduction in cell efficiency compared with those for a similar ideal loss-less cell at $K = 1000$.

For any given range of concentration values an advantageous grid design may be found. As a rule, the higher the cell conversion efficiency value, the more it decays with a change in K.

In contact grids of the kind discussed in this paper, the main ohmic power loss is related to the current flow through the radial metal fingers. However, most of the power loss (both ohmic and shading) takes place in the outermost region of the cell.

The number of collectors is an important parameter in grid design. For certain designs (*e.g.* type III at $K = 662$) an increase in the number of collectors beyond four hardly changes the efficiency whereas, in contrast, cells with an increased number of rings might be technologically advisable because one thick contact is more reliable than many thin contacts. In certain circumstances the number of thin metal fingers within a cell ring may be greatly reduced without much increase in the total power loss.

At 813 suns the cell efficiency is not a very sensitive function of the cell radius, but the cell output power is. An increase in the cell radius in real concentrator systems might be limited by thermal sinking or optics to a much greater extent than by cell power dissipation on the contact grid.

Acknowledgments

The authors thank Zh. I. Alferov for his constant interest in this paper and Drs. V. D. Rumiantsev and J. K. Aripov for valuable discussions and help with the experiments.

References

1 L. W. James and R. L. Moon, *Appl. Phys. Lett., 26* (5) (1975) 467.
2 Zh. I. Alferov, J. K. Aripov, B. V. Egorov, V. R. Larionov, V. D. Rumiantsev, O. M. Fedorova and L. Hernandez, *Fiz. Tekh. Poluprovodn., 14* (4) (1980) 685.
3 R. Sahai, D. D. Edwall and J. S. Harris, Jr., *Appl. Phys. Lett., 34* (2) (1979) 147.
4 Zh. I. Alferov, V. M. Andreev, J. K. Aripov, V. R. Larionov and V. D. Rumiantsev, *Geliotekhnika,* (6) (1981) 3.
5 E. Fanetti, C. Flores, G. Guarini, F. Paletta and D. Passoni, *Sol. Cells, 3* (1981) 187.
6 E. Fanetti, C. Flores, G. Guarini and F. Paletta, in W. H. Bloss and G. Grassi (eds.), *Proc. 4th Commission of the European Communities Conf. on Photovoltaic Solar Energy, Stresa, May 10 - 14, 1982,* Reidel, Dordrecht, 1982, p. 671.
7 P. E. Gregory, P. G. Borden, M. J. Ludowise, R. J. Owen, N. Kaminar, R. A. Larue and R. J. Boettcher, *Sol. Cells, 6* (1982) 103.
8 A. M. Allakhverdiev, B. V. Egorov, V. M. Lantratov and S. I. Troshkov, *Zh. Tekh. Fiz., 52* (11) (1982) 2312.
9 V. M. Andreev and O. V. Sulima, *Pis'ma Zh. Tekh. Fiz., 8* (7) (1982) 429.
10 A. Flat and A. G. Milnes, *Sol. Energy, 23* (4) (1979) 289.
11 M. Conti, *Solid-State Electron., 24* (1) (1981) 79.
12 J. K. Aripov and V. D. Rumiantsev, *Fiz. Tekh. Poluprovodn., 15* (4) (1981) 667.
13 K. W. Boer, *Sol. Energy, 19* (5) (1977) 525.

Appendix A

A.1. Derivation of eqn. (1)

In order to derive eqn. (1) let us assume that the current flowing towards the metal finger located between collectors p and $p - 1$ is collected from two A-type (Fig. A1, shaded region) portions of a solar cell.

As can be seen from Fig. A1, the current collected from the strip with a coordinate r, a width dr and an angle φ can be found to be

$$I(\varphi, r) = \int_0^{\varphi} KJ_L \, d\Omega \tag{A1}$$

where

$$d\Omega = d\varphi \, (r + dr)^2 - d\varphi \, r^2$$
$$\approx 2r \, d\varphi \, dr \tag{A2}$$

Substituting eqn. (A2) into eqn. (A1) gives

$$I(\varphi, r) = 2KJ_L r\varphi \, dr \tag{A3}$$

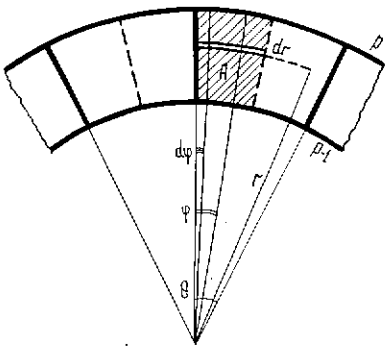

Fig. A1. Grid design element considered in the calculations.

The power drop due to current flow through this strip can be found to be

$$dP_s^A = \int_0^{\theta} I^2(\varphi, r)\rho_s \frac{r\, d\varphi}{h_s\, dr}$$

$$= \frac{4K^2 J_L^2 \rho_s \theta^3 r^3\, dr}{3h_s} \tag{A4}$$

It is evident that the power loss in the A-type part of the solar cell is given by

$$P_s^A = \int_{[(p-1)/m]R}^{(p/m)R} dP_s^A$$

$$= \frac{K^2 J_L^2 \rho_s \theta^3 R^4}{3h_s} \frac{p^4 - (p-1)^4}{m^4} \tag{A5}$$

and the power loss due to current flow through the semiconductor layer in the portion (ring) of the solar cell located between collectors p and $p-1$ normalized to the total power incident on the cell is given by

$$P_s = \frac{2N_p P_s^A}{KP_0 \pi R^2} \tag{A6}$$

As $\theta = 2\pi/2N_p$, eqn. (A6) can then be rewritten as eqn. (1).

A.2. Derivation of eqn. (2)

The normalized power loss due to current flow through the semiconductor–metal interface is given by

$$P_c = \frac{I^2 R_c}{KP_0 \pi R^2} \tag{A7}$$

where I is the collected current and R_c is the contact resistance given by

$$R_c = \frac{\rho_c}{h_m R/m} \tag{A8}$$

Considerations analogous to those used in the derivation of eqn. (A3) give an expression for the current collected from the A-type part of the solar cell (Fig. A1) which flows at the semiconductor–metal interface in the region of a radial finger:

$$I_A = \int_{[(p-1)/m]R}^{(p/m)R} 2KJ_L\theta r \, dr$$

$$= KJ_L\theta R^2 \frac{p^2-(p-1)^2}{2m^2} \tag{A9}$$

Then for the N_p radial fingers in the ring located between the collectors p and $p-1$ the normalized contact resistance power loss is

$$P_c = \frac{N_p(2I_A)^2R_c}{KP_0\pi R^2} \tag{A10}$$

The substitution of eqns. (A8) and (A9) into eqn. (A10) gives eqn. (2).

A.3. Derivation of eqn. (3)

In the derivation of eqn. (3) let us consider that the Joule loss P_{mi} due to current flow along a radial finger in the ring located between p and $p-1$ collectors is

$$P_{mi} = P_i + P_{2A} \tag{A11}$$

where P_i is the Joule loss due to the current I_i flow along a finger collected from the inner (relative to the ring under consideration) part of the solar cell and P_{2A} is the Joule loss due to the current I_{2A} flow along a finger collected from the two adjacent A-type parts (Fig. A1) of the solar cell. It is evident that the normalized P_i is

$$P_i = \frac{I_i^2R_m}{KP_0\pi R^2} \tag{A12}$$

where

$$I_i = \frac{KJ_L\pi\{R(p-1)/m\}^2}{N_p} \tag{A13}$$

and the metal finger resistance

$$R_m = \rho_m \frac{R/m}{h_m t_m} \tag{A14}$$

Substituting eqns. (A13) and (A14) into eqn. (A12) gives

$$P_i = \frac{KJ_L^2\pi R^3\rho_m(p-1)^4}{P_0N_p^2h_m t_m m^5} \tag{A15}$$

To obtain an expression for P_0 let us use the same approach as in the derivation of eqn. (A3). Thus an expression for the current collected from two A-type parts of the solar cell (Fig. A1) as a function of r can be written as

$$I_{2A}(r) = 2\int_{[(p-1)/m]R}^{r} 2KJ_L\theta r\,dr$$

$$= 2KJ_L\theta\left\{r^2 - \left(\frac{p-1}{m}\right)^2 R^2\right\} \tag{A16}$$

Then the normalized losses due to $I_{2A}(r)$ flow are

$$P_{2A} = \frac{1}{KP_0\pi R^2}\int_{[(p-1)/m]R}^{(p/m)R} \{I_{2A}(r)\}^2 \frac{\rho_m\,dr}{h_m t_m}$$

$$= \frac{4\rho_m KJ_L{}^2R^3\pi}{h_m t_m P_0 N_p{}^2}\,\frac{1}{m^5}\left[\frac{p^5-(p-1)^5}{5} - \frac{2(p-1)^2\{p^3-(p-1)^3\}}{3} + \right.$$

$$\left. + (p-1)^4\right] \tag{A17}$$

Then for the N_p fingers the Joule loss due to current flow along the metal fingers in the ring located between p and $p-1$ collectors is

$$P_m = N_p P_{mi} \tag{A18}$$

and substituting eqns. (A15) and (A17) into eqn. (A11) and then eqn. (A11) into eqn. (A18) we obtain eqn. (3).

A.4. Derivation of eqn. (4)

The normalized power loss within the cell due to the area shaded by the N_p fingers between collectors p and $p-1$ is

$$P_{sh} = \frac{S_{sh}}{S_{ring}}\,\frac{P_{ring}}{KP_0\pi R^2} \tag{A19}$$

where the surface of the area shaded by the N_p fingers is given by

$$S_{sh} = N_p\,\frac{h_m R}{m} \tag{A20}$$

the surface of the ring is given by

$$S_{ring} = \frac{\pi R^2}{m^2}\{p^2-(p-1)^2\} \tag{A21}$$

and the incident power on the ring is given by

$$P_{ring} = KP_0\,\frac{\pi R^2}{m^2}\{p^2-(p-1)^2\} \tag{A22}$$

Substituting eqns. (A20) - (A22) into eqn. (A19) we obtain eqn. (4).